Comparison of Regime Transition between Ellipsoidal and Spherical Particle Assemblies in a Model Shear Cell

M. Hossain, H. P. Zhu, A. B. Yu

Abstract—This paper presents a numerical investigation of regime transition of flow of ellipsoidal particles and a comparison with that of spherical particle assembly. Particle assemblies constituting spherical and ellipsoidal particle of 2.5:1 aspect ratio are examined at separate instances in similar flow conditions in a shear cell model that is numerically developed based on the discrete element method. Correlations among elastically scaled stress, kinetically scaled stress, coordination number and volume fraction are investigated, and show important similarities and differences for the spherical and ellipsoidal particle assemblies. In particular, volume fractions at points of regime transition are identified for both types of particles. It is found that compared with spherical particle assembly, ellipsoidal particle assembly has higher volume fraction for the quasistatic to intermediate regime transition and lower volume fraction for the intermediate to inertial regime transition. Finally, the relationship between coordination number and volume fraction shows strikingly distinct features for the two cases, suggesting that different from spherical particles, the effect of the shear rate on the coordination number is not significant for ellipsoidal particles. This work provides a glimpse of currently running work on one of the most attractive scopes of research in this field and has a wide prospect in understanding rheology of more complex shaped particles in light of the strong basis of simpler spherical particle rheology.

Keywords—Discrete element method, granular rheology, non-spherical particles, regime transition.

I. INTRODUCTION

REGIME transition is a unique phenomenon attributed to flow dynamics in the realm of granular rheology. Particle assemblies at dense condition subject to slow shear flow, which is known as quasistatic regime (e.g. [1]), is very different from particle assemblies that are more dilute subject to high flow conditions, which is recognized as inertial regime (e.g. [2]). There is an intermediate regime in between the two extreme regimes. Regime transition is that grey region where particle assembly exits from one regime to another. In the field of classical research of granular rheology, it is a complex issue that acts as an obstacle in the path of obtaining a simple numerical model similar to that of fluid mechanics. It is also responsible for creating significant complications in practical applications like bulk granular transportation and storage over a long period. Therefore, this subject has attracted special attention over the last decade [3]-[5] although it is far from the satisfactory grasp of the researchers in terms of knowledge that can allow a single constitutive general model to describe granular rheology across different regimes.

A popular device for studying regimes in granular flow is the shear cell [6]. Numerous works have been performed in a shear cell in order to understand this phenomenon (e.g. [7]-[9]). In the study of flow regimes, the key inputs often considered are: applied normal load on the test particle assembly by cell platens and the induced shear by platens moving in a direction perpendicular to the applied load. To study the regime transition of particle flow, Campbell [9], [10] defined three scaled parameters based on interrelationship between applied load, shear velocity, particle density, particle stiffness and particle diameter, which are a) elastically scaled stress, b) kinetically scaled stress and c) scaled stiffness. Based on the definitions, the transition point is where correlation curves for different scenarios collapse into a single curve. The method of identifying transition point using the correlation of the above mentioned parameters has been widely applied in the study of regime transitions (e.g. [3], [7]-[10]). However, the study was previously performed on spherical particle assemblies only and has not been conducted on non-spherical particles.

In this paper, a comparative research has been performed in a numerical platform using discrete element method (DEM) on spherical particle assembly and ellipsoidal particle assembly (where aspect ratio of ellipsoidal particles is 2.5:1) that are placed inside an annular shear cell in a pressure controlled (CP) environment. The elastically scaled stress, kinetically scaled stress, and coordination number are investigated with respect to volume fraction of the assemblies. It shows that, while the essential component of the finding, i.e. the collapse of correlation curves exists for both ellipsoidal and spherical particle assemblies, there are variations in the intricate details of the findings which motivate further research on the subject matter with respect to non-spherical particles. Further, relationship between coordination number and volume fraction at different flow conditions show different characteristics for the two types of particle assemblies.

M. Hossain is with the School of Computing, Engineering and Mathematics, Western Sydney University, Locked bag 1797, Penrith, NSW 2751, Australia (email: (18130049@student.westernsydney.edu.au).

H.P. Zhu is with the School of Computing, Engineering and Mathematics, Western Sydney University, Locked bag 1797, Penrith, NSW 2751, Australia (e-mail: h.zhu@westernsydney.edu.au).

A.B. Yu is with Faculty of Engineering, Monash University, 14 Alliance Lane (Engineering 72), Clayton Victoria 3168, Australia (e-mail: Aibing.Yu@monash.edu).

II. SIMULATION

The study is conducted with the DEM approach using commercial software Particle Flow Code (PFC3D). Soft particle simulation model is considered based on Hertz Mindlin & Deresiewicz force model [11]-[13].

An annular shear cell segment is generated across the flow for the investigation. The cubic segment is considered to be small enough to ignore the radius of curvature. All dimensions are scaled by particle diameter d to maintain universality of the findings. The size of the segment is 11d x 11d x h, where h is the height of the upper platen from the lower one that continuously adjusts itself to maintain constant pressure. This size is reasonable based on findings by Campbell [9], [10] (which suggests the size of the segment should be greater than 7d x 7d x 7d). Then, the upper platen and lower platen are constructed, with reasonable space in between them using 1d spherical particles glued together to a plate to create sufficient roughness for inducing shear effect. Walls perpendicular to the direction of flow (x-direction) are made using periodic boundaries such that a particle leaving one wall would immediately enter through the opposite wall with the same velocity, force, moment and y- and z-components of position. This is to ensure seamless continuity for infinite granular flow. The segment is illustrated in Fig. 1 for both the spherical and ellipsoidal particle assemblies. Next, 1,000 slightly poly-disperse specimen particles for investigation are randomly created in the empty space between the platens. Ellipsoidal particles are constructed with glued spherical particles using Bubble-pack algorithm so that their dynamic interactions are comparable with that of spherical particles. The other two side walls are made regular with minimum frictional resistance to flow to reduce the wall effect. Gravitational effect is ignored because a very large shear rate is required to obtain inertial regime as discussed in [9], which is practically not attainable. Similar consideration of overlooking gravitational effect was done in earlier work as well [7], [8]. The details of the particle properties assigned are given in Table I.

TABLE I
PARTICLE PROPERTIES AND PARAMETERS USED IN THE SIMULATIONS

Property	Value	Unit
Particle friction coefficient, μ	0.3	(-)
Critical damping ratio, D (normal and shear)	0.1	(-)
Young's modulus, E_y	2.5×10^6	$\pi \rho dg/6$
Poisson's ratio, ϑ	0.3	(-)
Time step	0.00001	$\sqrt{(d/g)}$
Normal pressure	0.05-7107.5	$\pi \rho dg/6$
Shear velocity	1.07-12.8	$\sqrt{(gd)}$

Once the setup is complete, the simulation is run to allow the assembly to relax and occupy the entire space naturally. Further, the two platens are moved in opposite direction at very low shear velocity to evenly distribute the particles in the confined space.

Now that it is ready, the upper platen continuously adjusts its position to impose pre-defined load on the specimen particle assembly. The shear velocity of the counter-moving platens is also gradually increased. At each of the data points, the simulation is run for a considerably long time to ensure steady state granular flow condition. Steady state condition is ascertained by following the trend of the upper platen's displacement. Once it shows only minor variation of upper platen's position around a constant value for a given set of conditions (load and shear rate) regardless of time, steady state condition is achieved.

Finally, the overall coordination number and volume fraction are obtained for individual data points for both spherical and ellipsoidal particle assemblies and correlated with scaled parameters: kinetically scaled stress, elastically scaled stress and scaled stiffness. The scaling methods are given below:

- Elastically scaled stress, $\sigma^* = \frac{\sigma d}{k}$

- Kinetically scaled stress, $\sigma' = \frac{\sigma}{\rho d^2 \dot{\gamma}^2}$

- Scaled stiffness, $k^* = \frac{\sigma'}{\sigma^*} = \frac{k}{\rho d^3 \dot{\gamma}^2}$

where σ, ρ, k and $\dot{\gamma}$ stands for applied stress, particle density, effective particle stiffness and platen shear velocity, respectively. How effective particle stiffness is obtained can be found elsewhere [3].
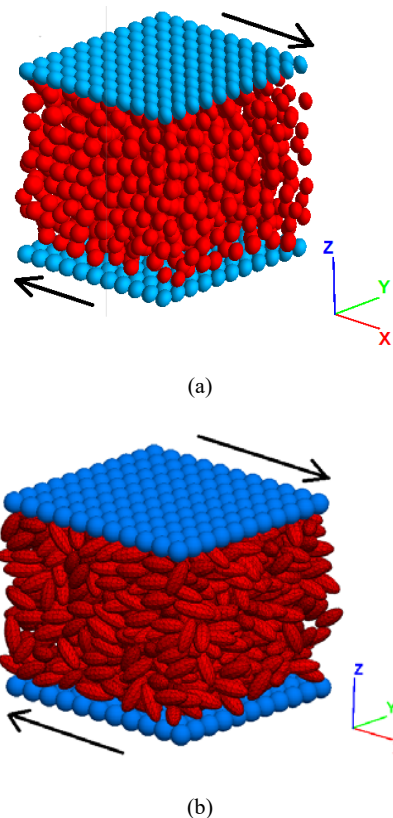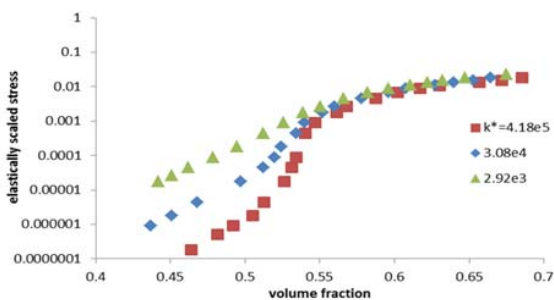

(a)

(b)

Fig. 1 Shear cell segments with (a) spherical particles and (b) ellipsoidal particles

III. RESULTS AND DISCUSSION

A. Correlation between Elastically Scaled Stress and Volume Fraction

Fig. 2 shows the comparative analysis of the dependence of σ^* on ν for different k^* for the spherical and ellipsoidal particle assemblies subjected to similar flow conditions. From Fig. 2 (a), it can be observed that the semi-log trend for the spherical particle assembly alluding to the quadratic relationship between σ^* and k^* is similar to that found in earlier studies, e.g. [3], [7], and [10]. At very low load ($\sigma^* < 5\times10^{-6}$), the compressibility of the assembly at the low shear rate ($k^* = 4.18\text{x}10^5$) is similar to that of the higher shear rate ($k^* = 3.08\text{x}10^4$), although corresponding load for the same stiffness is higher for the latter case. The intermediate applied load ($5\times10^{-6} < \sigma^* < 1\times10^{-3}$) is identified to be the crucial range of regime transition (also known as critical state concentration [10]) where the flow of spherical particles at low shear rate (or high k^*) demonstrate much lesser change of volume fraction with an increase of load. At very high shear rate ($k^* = 2.92\text{x}10^3$), this range is nearly invisible, where the volume fraction steadily increases with an increase of applied load. The critical point at which granular flow completely enters the quasistatic regime is established by the collapse of the three shear rate flow conditions into a single curve determining the independence of flow from the effect of varying shear rate (k^*). The corresponding volume fraction at the critical point is $\nu \approx 0.58$, which is the same as the one obtained in the previous studies [14].

(a)
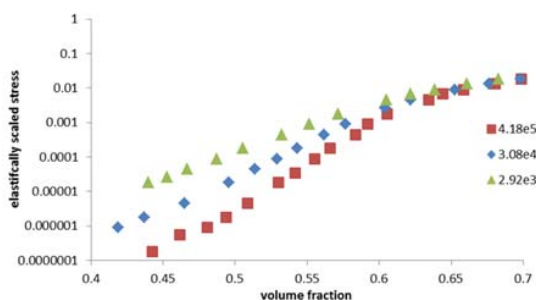
(b)

Fig. 2 Correlation between elastically scaled stress and volume fraction at different scaled stiffness for (a) spherical particles and (b) ellipsoidal particles of 2.5:1 aspect ratio

The ellipsoidal particle assembly in Fig. 2 (b) shows a partially different picture. The critical state concentration phenomena observed in the case of spherical particles is absent in the case of ellipsoidal particles. Independent of the shear rate (k^*), volume fraction steadily and quadratically increases with increase of applied load (σ^*) across all ranges of load. However, the correlation curves still maintain the important characteristic of collapsing into a single curve at high applied loads which is recognized as the point of regime transition into quasistatic regime. The collapsing point for ellipsoidal particles is found at volume fraction $\nu = 0.65$ beyond which the effect from variation of induced shear velocity by the platens is nullified.

This study proposes that the higher value of volume fraction at the transition point for the ellipsoidal particle assembly in the σ^*-ν curve with respect to that of the spherical particle assembly is a consequence of particle alignment of ellipsoidal particle flow which was well-established from earlier studies on non-spherical particles [14], [15]. The physical phenomenon is that the individual elongated particle tends to have its major axis parallel to the direction of granular flow. This enhances the compatibility of the ellipsoidal particle assembly more than spherical particle assembly at similar flow conditions.

The collapse of the multiple curves into a single one indicates that, at high load and in dense state, shear rate can no longer affect the flow at this state. At this stage, in practical situation, there exists individual particle deformation that significantly contributes to variation of the overall volume fraction of the assembly. Prior to this scenario, critical volume fraction (or critical concentration [10]) is observed in the case of spherical particles (Fig. 2 (a)) at the low shear rate ($k^* = 4.18\text{x}10^5$), where applied load is nearly independent of volume fraction: Increase in load (here, σ^*) has almost no change in volume fraction (ν). For the same assembly at the higher shear rate ($k^* = 3.08\text{x}10^4$, $2.92\text{x}10^3$), increase in the moment of inertia causes the rheological characteristics to drift from the critical volume fraction. But interestingly, for ellipsoidal particles, for the considered shear rates, the critical volume fraction does not exist (Fig. 2 (b)). This study suggests that it occurs because the alignment of particles in flow direction already provides a uniform structure in the flow which does not exist in the case of spherical particles. As a consequence, force transfer mainly occurs between gradient layers of ellipsoidal particles in a combined effect rather than individual particles. So, there is no change in trend observed for the same low shear rate ($k^* = 4.18\text{x}10^5$), the quasistatic state is approached at systematic graduation of assembly volume fraction even at low shear rates following expansion or compression of the assembly by layers.

B. Correlation between Kinetically Scaled Stress and Volume Fraction

Fig. 3 exhibits the variation of kinetically scaled stress σ' of the spherical and ellipsoidal particle assemblies with respect to change of volume fraction ν following previous work examples (e.g. [7]) in order to identify the point of regime

transition into inertial from intermediate states.

Fig. 3 (a) shows similar results to what is shown in earlier papers [3], [16] on spherical particles. The collapse of curves at lower σ' indicates the fact that σ' is insensitive to the shear rate (or k*) change. Since the term 'σ'' is already quadratically scaled, it complies with the definition of inertial regime proposed in earlier literature [9] which expresses σ' as a function of square of shear rate. At higher volume fraction, kinetically scaled stress is significantly affected by variation of shear rate (i.e. k*). In Fig. 3 (a), the point of regime transition to inertial state is found to be at ν = 0.51. On the other hand, Fig. 3 (b) shows the σ'-ν plot for different shear rate (k*) values for the ellipsoidal particle assembly. It is observed that the collapse of the σ'-ν curves at lower load distinguishing the inertial regime exists and the volume fraction at which the ellipsoidal particle assembly enters (or exits) the inertial regime is found to be 0.48. The dispersion of data at higher σ' for varying k* is relatively less, indicating that k* does not influence σ' for the ellipsoidal particle assembly as strongly as it does for the spherical particle assembly in the case of higher σ' values, which is similar to the effect of k* on σ*, as shown in Fig. 2. Moreover, the collapse of the σ'-ν curves for the ellipsoidal particle assembly occurs at σ' = 0.5 which is less than σ' = 1 for the spherical particle assembly, while the point of merging in the σ*-ν curves is nearly the same value of σ*(≈ 0.01) for both cases in Fig. 2. It is possible that particle shape has stronger influence in inertial regime with increase of sphericity of particles expediting inertial regime transition.

This study suggests that the lower value of volume fraction (0.48) for the ellipsoidal particle assembly in the σ'-ν curve compared to that of the spherical particle assembly (0.51) occurs due to the same physical phenomenon of preferential orientation which was mentioned earlier. The same reason may be applied to the study of inertial regime exit expedition (at σ' = 0.5) as discussed, because the laminar layers of the elongated particles reduces the possibility of random particle displacement in contrast with what is observed for spherical particles.

Another important feature in the study is the gap between the two identified points from the σ*-ν and σ'-ν curves. In our work, the volume fraction at the transition points identified are 0.51 (inertial regime) and 0.58 (quasistatic regime) for spherical particles which is similar to the information found in [9]. But for ellipsoidal particles, the data points have volume fraction of 0.48 and 0.65 for inertial and quasistatic regime transitions suggesting that there exists longer spread for the ellipsoidal particle assembly than that of the spherical one.

From a structural point of view, at low load and in a dilute condition, particle assembly mainly goes through continuous and random rearrangement of structure which is demonstrated in Fig. 3 by quadratic dependence of flow with shear rate. Unlike quasistatic regime, individual particle deformation at this stage is negligible. As the load increases and correspondingly volume fraction increases, the process of continuous random rearrangement is restricted by reduction of free path of particles. As a result, particle stress loses the

quadratic relationship with shear rate and hence we find that the single curve ceases to exist. In the case of ellipsoidal particles, random motion of the particles is further reduced by the alignment of the particles which was discussed in the previous section. So, in contrast to the finding for the case of spherical particles, the quadratic relationship between applied stress and shear rate ceases to exist much earlier at a lower volume fraction. And because of this pre-organized structure of ellipsoidal particles, the transition between trends at higher load condition and lower load condition is less distinct even for the low shear rates (k* = 4.18x10^5), unlike that of the spherical particle assembly.

Overall, it can be eluded from Fig. 2 and Fig. 3 that elongated particles have a relatively moderate transition point, while maintaining key principal characteristics of merger of correlation curves.
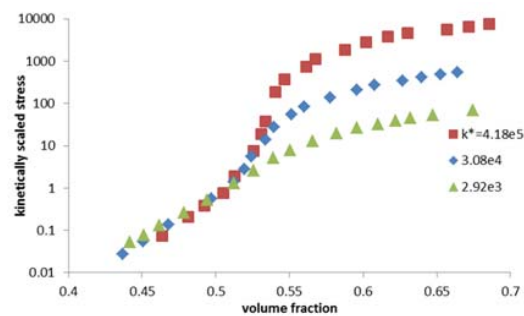
(a)
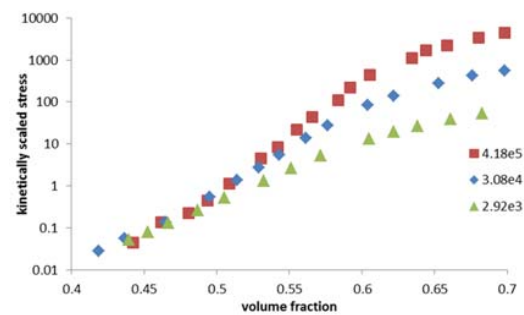
(b)

Fig. 3 Correlation between kinetically scaled stress and volume fraction at different scaled stiffness for (a) spherical particles and (b) ellipsoidal particles of 2.5:1 aspect ratio

C. Correlation between Coordination Number and Volume Fraction

Fig. 4 displays the relationship between overall coordination number and volume fraction of the particle assemblies at different flow conditions in terms of σ* and k*. Coordination number is obtained by the equation: $CN = \frac{2N_c}{N}$, where, N_c is the number of contacts and N is the number of particles. It has a clear differentiating element between the ellipsoidal and spherical particle assemblies. Fig. 4 (a) shows a similar relationship to Fig. 2 (a), as such that there exists of critical volume fraction for low shear rate (high k*) flow

condition at which the coordination number changes rapidly with little change in volume fraction. Again, it disappears as the shear rate increases (or k* decreases). It is in agreement with earlier literature [3]. Then, at higher volume fraction, the data collapse into a single curve. Coordination number for the ellipsoidal particle assembly is much higher than that of the spherical particle assembly. Similar observations were found in [14].

But a striking finding shows that there is very little change in the coordination number volume fraction relationship in the flow of ellipsoidal particles. It is the explicit depiction of the organized structure of ellipsoidal particles in the steady-state condition. However, there still exists a minor effect of induced shear with increasing shear rate (or decreasing k*), which marginally increases the overall coordination number which simply can be due to faster movement causing more rapid interaction of particles. It is worth mentioning that in all cases, there exists a positive relationship between coordination number and volume fraction which is in agreement with [17]. It is an interesting finding suggesting that relationship between coordination number and volume fraction may not be universally applicable.
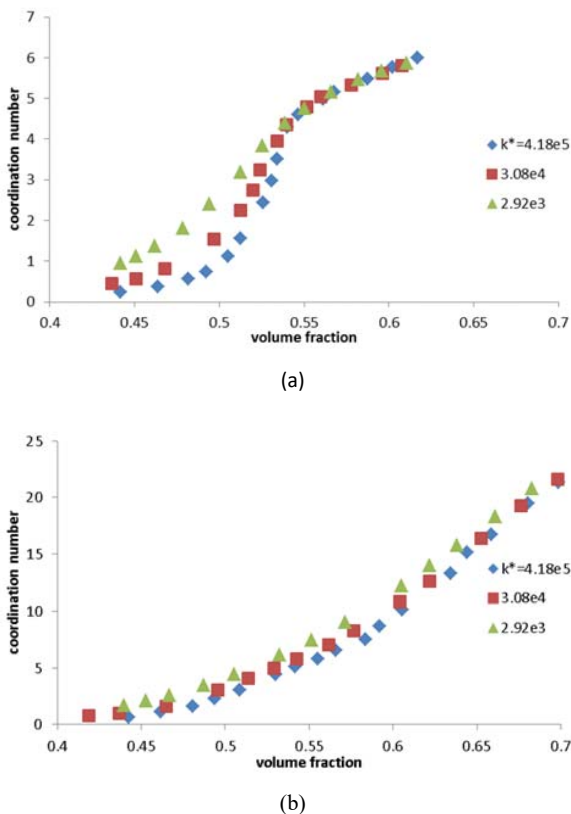

(a)

(b)

Fig. 4 Correlation between coordination number and volume fraction at different scaled stiffness for a) spherical particles and b) ellipsoidal particles of 2.5:1 aspect ratio

In an extension to the discussion in Section III*A* and III*B* in light of factual events, the stage regarding critical volume fraction region can be observed from Fig. 4 (a). At dilute condition, the compressibility of spherical particle assembly is high due to the abundant free path for particles. Thus, the volume fraction reduces without having much impact to the inertial regime-like contact network [3]. Once the capacity of compression of the assembly in its dilute state comes to the peak point, the process of continuous rearrangement of structure cannot be maintained any further and load bearing contact network starts building up rapidly (as seen in Fig. 4 (a)). On the other hand, for ellipsoidal particles, since the particle alignment causes the load to be propagated in layers, there is no distinguishing shift from random rearrangement of individual particles into the restricted dense state. As a consequence, shear rate does not affect the steady buildup of load bearing contact network with increase of applied pressure which is shown by the insensitivity of shear rate on coordination number variation with respect to volume fraction, as found in Fig. 4 (b).

IV. CONCLUSION

Ellipsoidal and spherical particle assemblies are sheared in a stress-controlled cubical segment of annular shear cell in a virtual environment by the application of discrete element method. In order to study regime transition, important parameters: Elastically scaled stress σ^*, kinetically scaled stress σ', coordination number and volume fraction v are investigated. The comparisons between the findings of the ellipsoidal particle flow and the spherical particle flow are carried out. Both the ellipsoidal and spherical particle assemblies show data collapse in the study of σ^*-v and σ'-v correlation curves, which is an important feature to identify points of regime transition. The points of regime transition for spherical particles are $v = 0.51$ (intermediate - inertial) and $v = 0.58$ (quasistatic - intermediate), which are similar to the results obtained in the previous studies. Compared with the spherical particle assembly, the ellipsoidal particle assembly has higher volume fraction for the quasistatic to intermediate regime transition ($v = 0.65$) and lower volume fraction for the intermediate to inertial regime transition ($v = 0.48$). The difference between two regime transition points obtained from the σ^*-v and σ'-v curves is larger for ellipsoidal particles. The dispersion of data at higher volume fractions in the study of the σ'-v curves is larger for the spherical particle flow relative to the ellipsoidal particle flow.

Critical state volume fraction (or concentration) exists for the spherical particles at lower shear rate, but is not found in the case of the ellipsoidal particle flow for the considered shear rates. An important difference is that coordination number is negligibly affected by the change of flow condition for the ellipsoidal particle flow, unlike what has been found for the spherical particle flow resembling σ^*-v curve study. The moderate regime transition for the ellipsoidal particle flow and their striking difference in the coordination number's dependence on volume fraction comes from the organized structure of these elongated particles through preferential orientation in the direction flow in steady state flow condition.

This paper proposes micro dynamic analysis of regime transition of non-spherical particle flow for future work.

REFERENCES

[1]   MiDia, "On dense granular flows," European Journal of Physics E-14, pp. 341-365, Aug. 2004.
[2]   R. Wildman, T. W. Martin, J. M. Huntley, J. T. Jenkins, H. Viswanathan, X. Fen and D. J. Parker, "Experimental investigation and kinetic-theory-based model of a rapid granular shear flow," Journal of Fluid Mechanics, vol. 602, pp. 63-79, 2008.
[3]   X. Wang, H. P. Zhu, S. Luding and A. B. Yu, "Regime transitions of granular flow in a shear cell: A micromechanical study," Physical Review, E-88 no. 3, pp. 032203, Sep. 2013.
[4]   M. Trulsson, B. Andreotti, and P. Claudin, "Transition from the viscous to inertial regime in dense suspensions," Physical review letters, vol. 109, no. 11, pp. 118305, Sep. 2012.
[5]   C. Heussinger, and J. L. Barrat, "Jamming transition as probed by quasistatic shear flow," Physical review letters, vol. 102, no. 21, p. 218303, 2009.
[6]   J. Carr and D. Walker, "An annular shear cell for granular materials," Powder Technology, vol. 1, no. 6, pp. 369-373, 1968.
[7]   L. Aarons and S. Sundaresan, "Shear flow of assemblies of cohesive granular materials under constant applied normal stress," Powder Technology, vol. 183, no. 3, pp. 340-355, Feb. 2008.
[8]   L. Aarons, and S. Sundaresan, "Shear flow of assemblies of cohesive and non-cohesive granular materials," Powder Technology, vol. 169, no. 1, pp. 10-21, July 2006.
[9]   C. S. Campbell, "Granular shear flows at the elastic limit," Journal of Fluid Mechanics, vol. 465, pp. 261-291, 2002.
[10]   C. S. Campbell, "Stress-controlled elastic granular shear flows," Journal of Fluid Mechanics, vol. 539, no. 1, pp. 273-297, 2005.
[11]   R. Mindlin, "Force at a point in the interior of a semi-infinite solid," DTIC Document, May 1953.
[12]   H. Hertz, "Hertz Theory (Uber die Beruhrung fester elastischer Korper)," Journal für die reine und angewandte Mathematik, vol. 92, pp. 156-171, 1881.
[13]   L. Vu-Quoc, X. Zhang, and O. Walton, "A 3-D discrete-element method for dry granular flows of ellipsoidal particles," Computer methods in applied mechanics and engineering, vol. 187, no. 3, pp. 483-528, 2000.
[14]   Y. Guo, C. Wassgren, B. Hancock, W. Ketterhagen, and J. Curtis, "Granular shear flows of flat disks and elongated rods without and with friction," Physics of Fluids (1994-present), vol. 25, no. 6, pp. 063304, June 2013.
[15]   M. Hossain, H. P. Zhu, A. B. Yu, "Microdynamic analysis of ellipsoidal particle flow in a shear cell," IV International Conference on Particle-based Methods – Fundamentals and Applications PARTICLES 2015, pp. 833-841, Oct. 2015.
[16]   S. Ji and H. H. Shen, "Internal parameters and regime map for soft polydispersed granular materials," Journal of Rheology (1978-present), vol. 52, no. 1, pp. 87-103, 2008.
[17]   X. Wang, H. P. Zhu, and A. B. Yu, "Microdynamic analysis of solid flow in a shear cell," Granular Matter, vol. 14, no. 3, p. 411-421, 2012.